

Estimation and control of vortex shedding at low Reynolds numbers

S. J. Illingworth

Department of Mechanical Engineering, University of Melbourne, VIC 3010, Australia

Abstract

This paper considers model-based estimation and control of the flow past a cylinder in low-Reynolds-number simulations. There are two parts to the study. The first part considers model-based control of the wake using a single velocity measurement as the feedback signal. Actuation is achieved using blowing and suction on the cylinder's surface. A reduced-order model is formed and used to design robust feedback controllers using modern control techniques. These robust controllers give rise to improved closed-loop performance, and are effective over a wider Reynolds number range than previously seen. As Reynolds number increases, however, single-sensor-based control becomes more challenging as the downstream extent of the absolutely unstable region increases. This motivates the second part of the study. Keeping with a single sensor measurement, we investigate how well one can estimate the entire flow field using only this single sensor. To do so, we use a Kalman filter, and excellent results are seen.

Introduction

The onset of the von Kármán vortex street in the two-dimensional cylinder wake is well-documented, the vortices first appearing at a Reynolds number near $Re = 49$ [20]. This vortex street gives rise to increased drag and unsteady lift forces. The advantages of suppressing these vortices is therefore clear, and the two-dimensional cylinder wake has become a canonical problem in flow control.

Active flow control schemes employ actuators to provide external energy to a fluid flow, thereby controlling it in some desired way. This actuation may be predetermined (open-loop), or may respond to some sensor measurement via some feedback law (closed-loop).

The earliest studies of closed-loop control of vortex shedding used a proportional feedback gain, whereby a sensor measurement at some point in the wake was multiplied by a scalar, proportional gain and fed back to give the control signal. The first such study was performed by Berger [1]. Vortex shedding, which occurred naturally for the oval-shaped cylinder at Reynolds numbers of 77 and above, was suppressed by feedback at Reynolds numbers up to 80. Proportional feedback control was also used by Roussopoulos [15] in his experimental study of a circular cylinder, and by Park *et al.* [11] in their numerical study. In both cases, vortex shedding was completely eliminated at Reynolds numbers slightly above that corresponding to the onset of vortex shedding.

In order to achieve better closed-loop control, more recent studies have used a wide range of control strategies including neural networks [4]; optimal control [5, 14, 2] and suboptimal control methods [10]; Linear-Quadratic-Gaussian (LQG) control [13]; and Proportional-Integral-Derivative (PID) control [16, 18].

In this paper, closed-loop control of the cylinder wake is investigated in direct numerical simulations at Reynolds numbers up to 100. The emphasis is on model-based control using reduced-order modelling techniques and robust control methods. After introducing the modelling and control methods used, we first

look at model-based control at a Reynolds number of 60. We demonstrate the superior performance of the model-based controller over the early trial-and-error-based proportional feedback control studies. We then look at control at $Re = 100$, and demonstrate the challenges of single-sensor-based control at this higher Reynolds number. Motivated by these challenges, we then design a dynamic estimator (a Kalman filter) for the wake, allowing us to estimate the entire flow field from a single sensor measurement.

Modelling and control of the cylinder wake

The flow is solved using direct numerical simulation. The spatial discretization is performed in cylindrical coordinates using an energy-conservative finite-difference scheme which is described in [3]. Time integration is performed using a low-storage third-order Runge-Kutta/Crank-Nicolson scheme. The computational grid has 256 points in the circumferential direction; 220 points in the radial direction (clustered near the cylinder surface); and extends 78 cylinder radii from the cylinder's centre. Numerical results have been validated using grid refinement and boundary placement studies, as well as comparison with experimental data. At Reynolds numbers between 60 and 100, the Strouhal numbers found agree with the experimental parallel-shedding data of Williamson [19] to within 1%.

We adopt the same feedback control arrangement as Park *et al.* [11] whose study, like this one, was numerical. The feedback arrangement is shown in figure 1. Sensing is provided by a probe positioned 2.75 cylinder diameters downstream of the cylinder's centre which measures the vertical velocity. Actuation is provided by anti-symmetrical blowing-and-suction at the cylinder's surface. The centres of the two actuation regions are located at angles of $\pm 70^\circ$ from the cylinder's downstream-pointing horizontal, and their distribution is Gaussian, specified such that the amplitude has fallen to 1% of its peak at an angle of $\pm 25^\circ$ from its centre.

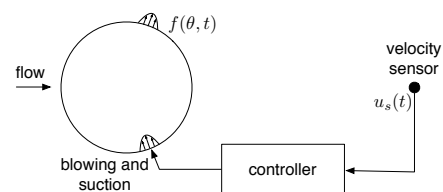


Figure 1: Feedback control arrangement.

In order to design feedback controllers, we first require a reduced-order model of the cylinder wake. This can be achieved by forming a state-space model of the form

$$\dot{x}(t) = Ax(t) + Bu(t) \quad (1a)$$

$$y(t) = Cx(t), \quad (1b)$$

where $u \in \mathbb{R}^p$ is a vector of inputs; $y \in \mathbb{R}^q$ is a vector of outputs; $x \in \mathbb{R}^n$ is the system state; and A , B and C are suitably-dimensioned matrices. The feedback arrangement, shown in figure 1, has a single input, $p = 1$, and a single output, $q = 1$.

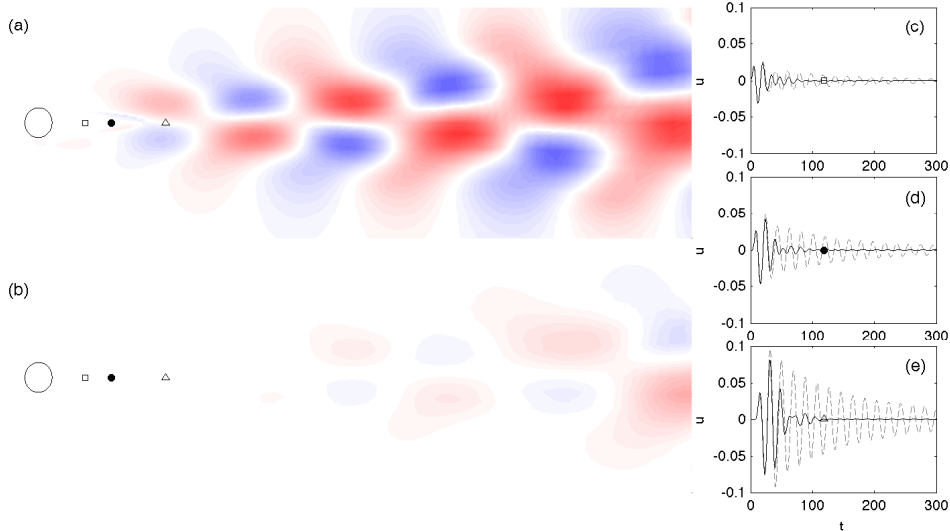


Figure 2: Control at $Re = 60$: control with (a) a proportional feedback gain; and (b) a model-based controller; (c-e) transverse velocity at three locations, which are indicated in parts (a,b). The measurement used for control is shown in (d).

We use the Eigensystem Realization Algorithm (ERA) to form a reduced-order model. The ERA uses a system’s impulse response—found in the cylinder’s case directly from simulation data—to form a Hankel matrix, which is closely linked to the system’s observability and controllability Gramians. These Gramians can be obtained after performing a singular value decomposition of the Hankel matrix. The ERA produces reduced-order models which are balanced, the balancing referring to their observability and controllability Gramians being equal and diagonal. Physically this means that the input-output behaviour of the system is properly captured, and this is important for feedback control purposes. For more details on the ERA, see [8, 7], and for its application to flow control, see [9, 6].

Model-based control at $Re = 60$

We first look at control at a Reynolds number of 60. Since the wake is unstable at this Reynolds number, it is difficult to find a linear, reduced-order model. We therefore first find a reduced-order model at $Re = 45$, for which the wake is stable; design a feedback controller for this Reynolds number; and apply the controller at $Re = 60$. Since robust control methods are used (specifically, \mathcal{H}_∞ loop-shaping), the controller is sufficiently robust that it achieves closed-loop stability when applied at $Re = 60$. Results are shown in figure 2, where the model-based controller is compared to control with a proportional feedback gain like that used by Park *et al.* [11]. This proportional gain was optimized over a range of values, and hence represents the best that could be found. The model-based controller provides better attenuation not only at the sensor location (figure 2c), but also better attenuation in the entire domain (shown at a particular instant in time in figure 2a,b).

Model-based control at $Re = 100$

We now look at control at a higher Reynolds number of 100. Figure 3 shows the wake’s closed-loop impulse response using a feedback controller which was designed for this Reynolds number. (Again, the controller has been designed using \mathcal{H}_∞ loop-shaping methods.) Figure 3 highlights the challenges of control at this higher Reynolds number: although the controller achieves good suppression at the sensor location (which is what it sets out to achieve), significant unsteadiness still exists downstream of the sensor. This is reasonable: The convective nature of the wake means that the controller is unaware of what is hap-

pening downstream of the sensor, and since it is unaware of this downstream unsteadiness, it cannot possibly do anything about it. This is borne out in parts (c) and (e) of figure 3, which show the time variation of the sensor measurement and of the blowing-and-suction actuation, respectively. The controller suppresses oscillations at the sensor location quite effectively and, once it has done so, the control signal remains small: as far as the controller is concerned, there is very little left to suppress. This phenomenon emerges at higher Reynolds numbers because the wake’s region of absolute instability extends further downstream [12]. The consequence is that single-sensor-based control is not suitable at these higher Reynolds numbers. This in turn motivates the next and final section, where we attempt to use our single sensor measurement, together with a reduced-order model of the wake, to estimate the entire flow field.

Estimation problem at $Re = 45$

One way to address the larger region of absolute instability seen in the previous section would be to place the single sensor further downstream. While this certainly provides better information about the far wake, it also introduces a problem of its own: a larger time delay in the control loop. With the sensor further downstream, the time taken for information from the cylinder (where disturbances that need to be controlled are likely to be generated) to propagate to the sensor location increases, and this has an adverse effect on control [17]. There is therefore a trade-off between the size of the time delay and the information retrievable from the far wake when a single sensor is used. A natural alternative would be to use two or more sensor locations for control. Then sensors near the cylinder would provide relatively new information, whilst those further away would provide information about the far wake. This is not particularly practical, though, and so an alternative is sought.

In this section we continue to measure at the same location with a single sensor. Motivated by the results of the previous section, we now investigate how well one can estimate the entire flow field using this single sensor measurement. This is an important question because if we can estimate the entire flow field sufficiently well with a single sensor, and then perform control actions based on this estimate, then we should be able to overcome the difficulties encountered at higher Reynolds numbers without requiring any additional sensors. As a first step towards

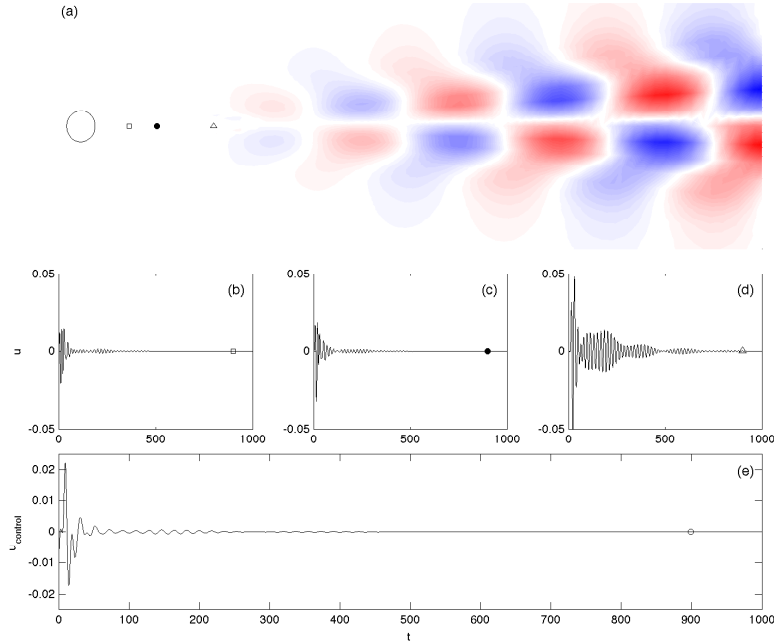


Figure 3: Control at $Re = 100$: (a) flow field at a particular instant, which is marked in parts (b-e); (b-d) transverse velocity at three locations, which are indicated in part (a). The measurement used for control is shown in (c), and (e) shows the feedback control signal.

this goal, we investigate the estimation problem at a Reynolds number of 45. We require two things to perform the estimation problem. The first is a suitable reduced-order model. The second is a dynamic estimator.

In the previous sections, we were interested in only a single sensor measurement, and so our model had a single input and a single output (see figure 1). In this section, we still have a single input, but the output—the entire flow field—is of much higher dimension. There are 220 grid points in the radial direction and 256 grid points in the circumferential direction, which together make for 56320 output locations. This is not tractable. We might decide to restrict our attention to a particular part of the domain, but even then we will have of the order of tens of thousands of outputs. To make the problem tractable, we reduce the number of outputs by computing their leading POD modes. We still use the ERA to find the reduced-order model. The procedure to find the reduced-order model is as follows. Perform an impulse response simulation as before, taking the entire field as the outputs; compute the leading POD modes of these outputs; and use the time-varying POD coefficients as the output used by the ERA. Due to the high dimension of the full field, we use the method of snapshots to compute the POD modes. We use 27 POD modes, which is sufficient to capture 99.99% of the energy in the wake’s impulse response. Using the POD coefficients, together with the single sensor location, as our output, we have a total of $27 + 1 = 28$ outputs.

Our task now is to estimate the 27 POD coefficients using only values of the velocity at our sensor location. We can achieve this using a dynamic estimator, which is often referred to as an *observer* or simply an *estimator* in the control community. For a state-space model of the form (1), an observer uses knowledge of the input, $u(t)$, and of the output, $y(t)$, to determine an estimate of the state, $\hat{x}(t)$, and an estimate of the output, $\hat{y}(t)$, using

$$\hat{\dot{x}}(t) = A\hat{x}(t) + Bu(t) + L[y(t) - \hat{y}(t)] \quad (2a)$$

$$\hat{y}(t) = C\hat{x}(t). \quad (2b)$$

This system mimics the original state-space model (1), but is also forced by the output error $[y(t) - \hat{y}(t)]$ via the observer gain matrix L . We will use a specific type of observer: the Kalman filter, which amounts to a particular choice of the observer gain matrix L . This choice of L is optimal in the sense that the error converges in the presence of stochastic disturbances d and measurement noise n , which are each assumed to be zero-mean, Gaussian, white-noise processes. (We add disturbances d to the control signal, and noise n to the sensor measurement in this section.)

Results of the estimator for the $Re = 45$ wake are shown in figure 4. Even in the presence of unknown disturbances, d , and measurement noise, n , the Kalman filter performs remarkably well in estimating the full flow field. This is demonstrated in figure 4 for a region of the full flow at a particular instant in time; and as a function of time at three specific points in the flow.

Conclusions

This study has considered the estimation and control of the cylinder wake at low Reynolds numbers. In the first part, model-based control using a single sensor measurement has been considered. This single sensor acts both as the feedback signal and as the quantity to be controlled. At a Reynolds number of 60, the model-based controller performs significantly better than a trial-and-error-based proportional feedback gain. Furthermore, the model-based control approach eliminates vortex shedding at a higher Reynolds number of 100. However, control at this higher Reynolds number is more challenging with a single sensor, owing to the larger region of absolute instability. Simply placing the sensor further downstream will help to alleviate this problem, but introduces problems of its own. In particular, the convective nature of the flow means that a sensor placed too far downstream introduces a time delay which is unacceptably large. These challenges with single-sensor-based control helped motivate the second part of the study, which looked at the estimation of the full flow field using a single sensor measurement. To achieve this a Kalman filter was used, and excellent results

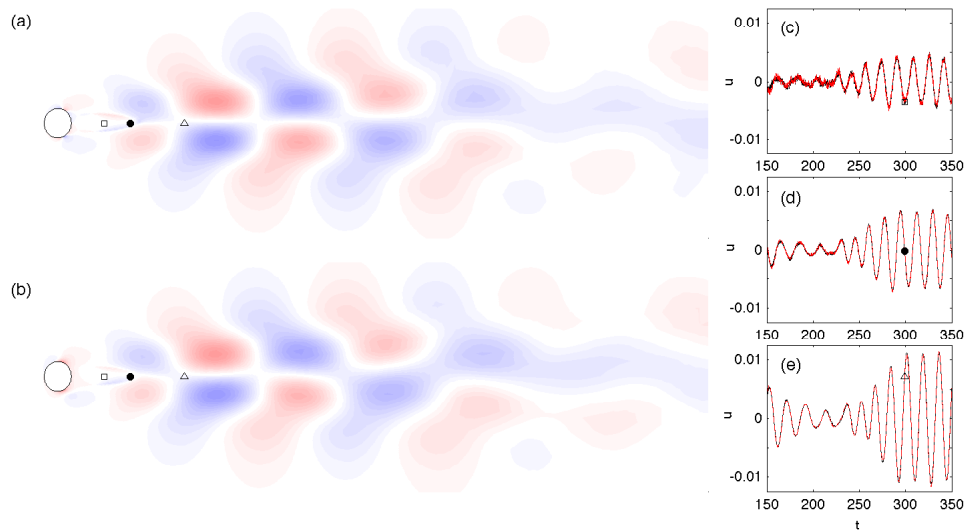


Figure 4: Estimation of the flow field at $Re = 45$: (a) the true flow field; and (b) the estimated flow field at a particular instant in time. (c-e) show the transverse velocity at the three locations indicated in (a,b). Both the true (—) and estimated values (---) are shown. (Notice that the measured velocity in (d), despite being measured, is also estimated.)

were seen. The natural next step is to use an estimator-based control scheme, where the estimated flow field is used as the input to the feedback controller. In this case a single measurement is still used for control. However, it distinguishes itself from the control schemes considered in this paper in one important way: that the control actions are based on (the estimate of) what is happening in the full domain.

References

- [1] Berger, E., Suppression of vortex shedding and turbulence behind oscillating cylinders, *Phys. Fluids Suppl.*, **10**, 1967, S191–S193.
- [2] Bergmann, M., Cordier, L. and Brancher, J.-P., Optimal rotary control of the cylinder wake using proper orthogonal decomposition reduced-order model, *Phys. Fluids*, **17**, 2005, 097101.
- [3] Fukagata, K. and Kasagi, N., Highly energy-conservative finite difference method for the cylindrical coordinate system, *J. Comput Phys.*, **181**, 2002, 478–498.
- [4] Gillies, E. A., Low-dimensional control of the circular cylinder wake, *J. Fluid Mech.*, **371**, 1998, 157–178.
- [5] Graham, W. R., Peraire, J. and Tang, K. Y., Optimal control of vortex shedding using low-order models. Part II—model-based control, *Internat. J. Numer. Methods Eng.*, **44**, 1999, 973–990.
- [6] Illingworth, S. J., Morgans, A. S. and Rowley, C. W., Feedback control of flow resonances using balanced reduced-order models, *J. Sound Vib.*, **330**, 2011, 1567–1581.
- [7] Juang, J. N., *Applied System Identification*, Prentice Hall, 1994.
- [8] Juang, J. N. and Pappa, R. S., An Eigensystem Realization Algorithm for modal parameter identification and model reduction., *J. Guid. Contr. Dyn.*, **8**, 1985, 620–627.
- [9] Ma, Z., Ahuja, S. and Rowley, C. W., Reduced order models for control of fluids using the Eigensystem Realization Algorithm, *Theor. Comp. Fluid Mech.*, **25**, 2011, 233–247.
- [10] Min, C. and Choi, H., Suboptimal feedback control of vortex shedding at low Reynolds numbers, *J. Fluid Mech.*, **401**, 1999, 123–156.
- [11] Park, D. S., Ladd, D. M. and Hendricks, E. W., Feedback control of von Kármán vortex shedding behind a circular cylinder at low Reynolds numbers, *Phys. Fluids*, **6**, 1994, 2390–2405.
- [12] Pier, B., On the frequency selection of finite-amplitude vortex shedding in the cylinder wake, *J. Fluid Mech.*, **458**, 2002, 407–417.
- [13] Protas, B., Linear feedback stabilization of laminar vortex shedding based on a point vortex model, *Phys. Fluids*, **16**, 2004, 4473–4488.
- [14] Protas, B. and Styczek, A., Optimal rotary control of the cylinder wake in the laminar regime, *Phys. Fluids*, **14**, 2002, 2073–2087.
- [15] Roussopoulos, K., Feedback control of vortex shedding at low Reynolds numbers, *J. Fluid Mech.*, **248**, 1993, 267–296.
- [16] Siegel, S., Cohen, K. and McLaughlin, T., Numerical simulations of a feedback-controlled circular cylinder wake, *AIAA J.*, **44**, 2006, 1266–1276.
- [17] Skogestad, S. and Postlethwaite, I., *Multivariable Feedback Control: Analysis and Design*, Wiley, 2005.
- [18] Son, D., Jeon, S. and Choi, H., A proportional-integral-differential control of flow over a circular cylinder, *Phil. Trans. R. Soc. A*, **369**, 2011, 1540–1555.
- [19] Williamson, C. H. K., Oblique and parallel modes of vortex shedding in the wake of a circular cylinder at low Reynolds numbers, *J. Fluid Mech.*, **206**, 1989, 579–627.
- [20] Williamson, C. H. K., Vortex dynamics in the cylinder wake, *Annu. Rev. Fluid Mech.*, **28**, 1996, 477–539.